

Journal of Photonics for Energy

SPIDigitalLibrary.org/jpe

Enhancement of quality of downconverted white light

Debasis Bera
Sergey Maslov
Lei Qian
Paul H. Holloway

Enhancement of quality of downconverted white light

Debasis Bera, Sergey Maslov, Lei Qian, and Paul H. Holloway

University of Florida, Department of Materials Science and Engineering,
Gainesville, Florida 32611-6400

debasis.bera@philips.com

Author is currently working at Philips Lumileds, 370 West Trimble Road, San Jose,
California 95131

Abstract. High-quality downconverted white light is important for many applications, including general illumination. Downconversion of blue light from inorganic InGaN-based light emitting diodes to produce white light is demonstrated using red- and green-emitting phosphors. After characterization, films of the phosphors are prepared by mixing the powder into a polymethyl methacrylate host. The quality of light is improved and optimized by varying the weight ratio of green to red phosphors and the thickness of the phosphor layer. © 2011 Society of Photo-Optical Instrumentation Engineers (SPIE). [DOI: [10.1117/1.3555421](https://doi.org/10.1117/1.3555421)]

Keywords: downconversion of blue to white light; color rendering index; color coordinates; color temperature; white light efficacy; light-emitting diodes.

Paper 10106R received Jun. 24, 2010; revised manuscript received Dec. 8, 2010; accepted for publication Jan. 25, 2011; published online Mar. 14, 2011.

1 Introduction

Ever since the concept of downconversion of blue light from a light-emitting diode to white light was introduced,¹ improving the quality of the white light has been a prime focus of solid state lighting research. The research emphasized many different areas, including research on phosphors.²⁻⁵ Two measures of the quality of the white light⁶ are the color-rendering index [(CRI) or Ra] and the correlated color temperature (CCT). For general lighting applications, Ra values approaching 100 represent high-quality white light and generally correspond correlated with CCTs in the range of 3000–6000 K. Another measure of color is the (x,y) chromaticity coordinates from the Commission Internationale de l'Eclairage (CIE) diagram, and a good white should have values close to (0.33, 0.33).

White light can be generated by two or three complementary wavelengths of light because there are three types of color-sensitive receptors in the human eyes. Complementary colors (e.g., blue and yellow) have been used to generate a white light. Guo et al.⁷ demonstrated that an efficiency of 326 lm/W and CIE chromaticity coordinates of (0.31, 0.32) could be achieved using a bichromatic blue and yellow distribution, where a full width half maxima (FWHM) of both the blue and yellow peaks were 5 nm. However, the Ra value was very low at 10. When the blue and yellow peaks were broadened to FWHMs of 20 nm, Ra increased to 26, but the efficiency decreased to 306 lm/W. In other words, the luminance efficiency was enhanced at the expense of the CRI values. Because the quality of the white light is an important criterion for general purpose lighting, a significant amount of research has been devoted to broadening⁸ and shifting⁹ the blue and yellow peaks in a bichromatic system. Two phosphors emitting at green and red wavelengths¹⁰⁻¹² can generate high-quality white light in a trichromatic system. However, different rates of aging for red and green phosphors often result in changes of color coordinate with time. In addition, the inorganic light-emitting diode (iLED) operates at temperature as high as 120°C,¹³ which may lead to thermal quenching¹⁴ and low quantum yield. Therefore, stability

at high temperatures and high T_c for thermal quenching are important properties of phosphors. Alternatively, the phosphor layer can be remote from the p - n junction of the iLED.

In the present study, we used red and green phosphors with the same composition and polymethylmethacrylate (PMMA) host to downconvert blue light from an iLED to produce white light. The phosphor layer was a few millimeters away from the iLED die to minimize thermal quenching. The weight ratio of green and red phosphors to maximize the quality of the white light was determined.

2 Characterization of Phosphors

Two sulfoselenide-based phosphor-doped [with a green (PG) and a red (PR)] emitters were received from PhosphorTech (Lithia Springs, USA). The particle size distributions of the PG and PR phosphors were characterized by dynamic light scattering (Honeywell, model UPA 150) with the particles dispersed in water by 15 min of ultrasonication. A JEOL JSM 6400 scanning electron microscope (SEM) was used for morphological characterization of the phosphors. Samples for the SEM were prepared by pressing the phosphor powders onto a Cu tape, followed by a thin coating of sputter-deposited carbon to reduce charging. Solid state photoluminescence (PL) and PL excitation (PLE) spectra from the phosphors were acquired using a monochromatized Xe excitation source (JASCO FP 6500). Different amounts of green to red phosphor were weighed and dispersed in anhydrous ethanol with weight ratios of green to red of 1:2, 1:1, 2:1, 3:1, and 4:1. The mixtures were ultrasonicated before PL analysis in a spectrophotometer (Horiba JobinYvan Fluoro-Max 3). During PL data acquisition, all optics and settings were kept same. The solid state CIE color coordinates and quantum yields (QYs) of thin-films were determined using a JASCO FP6500 spectrophotometer, software for data reduction, and integrating sphere. The room-temperature optical characteristics of blue light from the iLEDs and downconverted white light from the device plus phosphor layer were determined using a SpectraScan PR650 camera (PhotoResearch).

For QYs, the phosphor powders were deagglomerized and sandwiched between two thin (0.25-mm) glass substrates. The QYs of the phosphor films were calculated using

$$\Phi_{\text{PL}} = \frac{E_{\text{direct}} - \left(1 - \left[\frac{EX_{\text{secondary}} - EX_{\text{direct}}}{EX_{\text{secondary}}}\right]\right) E_{\text{secondary}}}{\left[\frac{EX_{\text{secondary}} - EX_{\text{direct}}}{EX_{\text{secondary}}}\right] EX_{\text{empty}}}, \quad (1)$$

where EX_{empty} , EX_{direct} , and $EX_{\text{secondary}}$ are integrated excitation intensities for two blank glass slides, and for a phosphor sample with direct and indirect excitation, respectively. E_{direct} and $E_{\text{secondary}}$ are the PL emission from the phosphor using direct and indirect excitation, respectively. The indirect emission was measured with the sample inside the integrating sphere but not in the direct path of the excitation light. Secondary emission is due to reflected excitation light subsequently absorbed by the sample.

3 Preparation of Phosphor Films on Inorganic Light-Emitting Diodes

PMMA was used as a host to create phosphor films. The glass-transition temperature of PMMA with a molecular weight 950,000 was reported to be $\sim 125^\circ\text{C}$.¹⁵ The refractive index of the PMMA-chlorobenzene solution was 1.52 at 380 nm and 1.49 at 780 nm. The phosphors/PMMA solutions were stirred for 30 min at room temperature. To optimize the composition of the phosphor layers, a concentration of phosphor in the PMMA/chlorobenzene solution of 100 mg/ml was used. The weight ratios of green to red phosphors in the 100 mg phosphor per milliliter of solution were varied from 1:1, 2:1, 3:1, and 4:1 and will be labeled as GR11, GR21, GR31, and GR41, respectively.

Four InGaN iLEDs with an emission peak near 475 nm were used as light-excitation sources. The polymeric encapsulant domes of these iLEDs were ground flat and polished to create a surface that was parallel to InGaN die surface. The area of the polished flat was constant

($5 \times 10^{-5} \text{ m}^2$) for all samples. A 50- μL volume of phosphor-PMMA solution was directly coated onto the polished flat, minimizing the number of interfaces to scatter light (refractive index of the iLED encapsulant was $\sim 1.50^{16}$). A control sample (PR00) was prepared by depositing 50 μL of PMMA-chlorobenzene solution without phosphor onto a polished flat iLED surface. The coated iLED samples were placed upright and dried for 1 h in flowing room-temperature air. The dried phosphor film on iLED was characterized using an optical microscope. Average thickness of film prepared from 50- μL phosphor-PMMA mixtures was found to be 90 μm . Optical microscopic analyses showed a compact film of phosphors on the encapsulant dome. The top surface of dried PMM-phosphor film was found to be smooth. When a control sample was optically investigated, a clearer view of the LED die inside the encapsulant dome was observed from the PMMA-deposited top compared to a polished-only encapsulant iLED. This is due to a refractive index match between encapsulant and PMMA.

4 Setup for iLED Downconversion Study

The InGaN iLEDs used as a blue light source had an emission peak at $\sim 475 \text{ nm}$, as shown Fig. 1(a). Figure 1(b) shows the typical I - V characteristics of these iLEDs over the range of 2–3.2 V. Fig. 1(c) shows that the 1931 CIE color coordinates changed from (0.127, 0.117) at driving voltage of 2.35 V to (0.125, 0.85) at 2.95 V. These changes, although relatively small, were due to an increased FWHM and a blueshift of the iLED peak maxima with increasing power to the iLED.¹⁷ Figure 1(d) shows luminance (candela per square meter) versus applied power to an iLED with a polished flat. As discussed above, the luminance of iLEDs was acquired using a calibrated PR650 (PhotoResearch) camera. The luminance was measured in a normal direction to the surface with a focal-plane spot diameter of 2 mm at the camera focal distance.

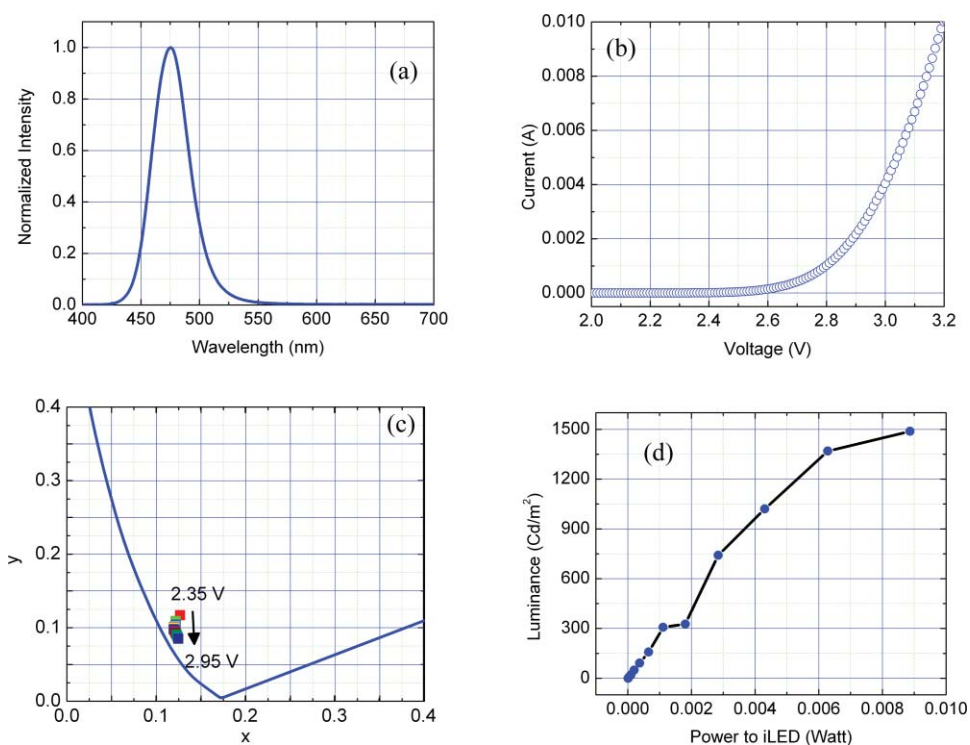


Fig. 1 (a) Electroluminescent spectra from an iLED at 2.4-V driving voltage, (b) I - V characteristics of a typical iLED, (c) expanded 1931 CIE diagram showing the shift of the CIE coordinates versus voltage to the iLED, and (d) luminance versus power of iLED.

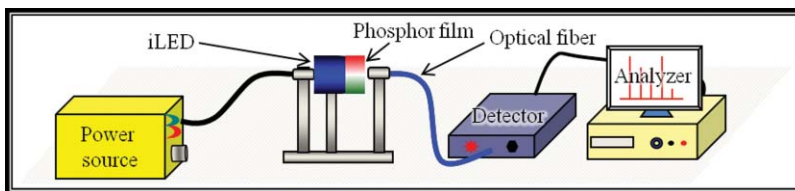


Fig. 2 Instrumental setup for photoluminescence measurement.

The emission from the iLED was forward focused to within 10 deg of the surface normal. A luminance of 1500 cd/m² was measured at a voltage of 2.95 V and current of 0.00301 A.

A customized instrumental setup for collecting downconverted light from the iLED, shown in Fig. 2, consists of four main parts: (a) a dc power supply for the iLED (Keithley 238 ammeter), (b) holders to support iLEDs and optical fiber for collecting the luminescent spectra, (c) a silicon charged-coupled detector (Ocean Optics), and (d) software to acquire (OOIBase 32 ver.2.0 Ocean Optics) and analyze (Spectra Manager, JASCO) the data.

5 Result and Discussion

5.1 Particle-Size Analysis

Downconversion depends on size distribution, morphology, and shape of the particles, because the scattered light intensity per particle is proportional to the sixth power of the diameter of the particle, according to the Rayleigh scattering theory.¹⁸ The phosphor particle-size distribution was determined by dynamic light scattering, as shown in Figs. 3(a) and 3(b) for the PG and PR phosphors, respectively. The mean particle size by volume (m_v) was 2.77 μm and by number (m_n) was 2.54 μm for the green-emitting phosphor. For the PR phosphor, the values of m_v and m_n were 2.98 and 1.99 μm , respectively. As shown, the PR phosphor has a broader distribution of particle size compared to the PG phosphor, and the smallest particle size of the PR phosphor was $\sim 1 \mu\text{m}$.

The dynamic light-scattering data reported above are for particles dispersed in water, whereas the downconversion particles were powders dispersed in a solid host. Figure 4 shows SEM images of the PG and PR dried phosphor particles. The size of some dried PG phosphor particles was as large as 50 μm , as shown in Fig. 4(a). High-resolution SEM images show that these large particles were agglomerated small particles. The largest agglomerated PR particles, on the other hand, were smaller (25 μm), as shown in Fig. 4(b), even though the particle-size distribution of the PR was larger than that of PG phosphor.

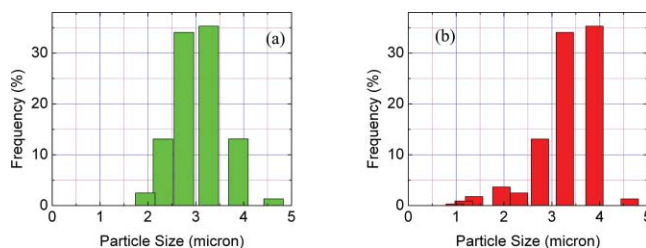


Fig. 3 Particle size distributions of (a) PG phosphor and (b) PR phosphor as determined by dynamic light scattering.

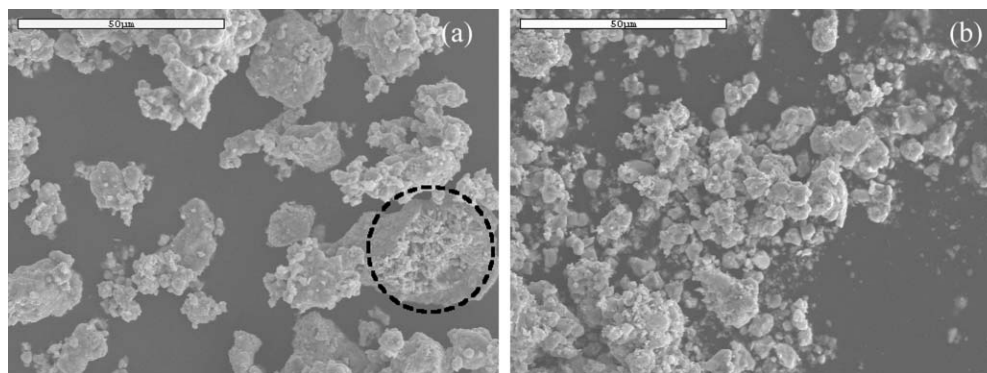


Fig. 4 SEM images of dried (a) green-emitting phosphor (PG) and (b) red-emitting phosphor (PR). The dotted circle in (a) shows that the large agglomerated particles are composed of small particles. (Scale bar: 50 μm).

5.2 Photoluminescence Study

The PL and PLE spectra of the PG and PR phosphors are shown in Fig. 5(a). The PL spectra from the PG and PR phosphors had maxima at 535 and 610 nm, and FWHM of ~ 50 and ~ 65 nm, respectively. When the samples were excited with 460 nm or at the PLE peak maxima, neither the PL peak position nor FWHMs changed values. Optical properties of the two phosphors are summarized in Table 1.

Note that the PLE spectra of the PG and PR phosphors overlap quite well in the region between 400 and 500 nm. Therefore, light in that wavelength range will excite both the green and red phosphors, simultaneously. The source of excitation was an iLED with an emission peak centered at 478 nm, which excited both the red and green phosphors. There is also a significant overlap between the PLE spectrum of PR and the PL emission spectrum of PG phosphors, as shown in Fig. 5(a). Therefore, a significant fraction of the PG green emission was absorbed by the PR phosphor.

In order to determine the appropriate ratio of green to red phosphors, mixtures with different weight ratios of PG and PR were prepared in anhydrous ethanol. Figure 5(b) shows the normalized PL spectra (excited at 460 nm) from samples with weight ratios of PG to PR of 1:2 (GR12), 1:1 (GR11), 2:1 (GR21), 3:1 (GR31), and 4:1 (GR41). As expected, the intensity of the red emission peak was more than two times higher than the green emission peak for the sample GR12. For the GR11 sample, the enhancement was ~ 1.5 times, although the weight ratio or green to red phosphor was 1:1. Consequently, a gradual but nonlinear decrease of the red emission peak relative to the green was observed with increased weight ratios of the PG to PR phosphor. Curve fitting on the trace of diminishing red peak intensity (y) versus increase in weight ratio of green to red phosphor (x) fit the following expression with a regression value

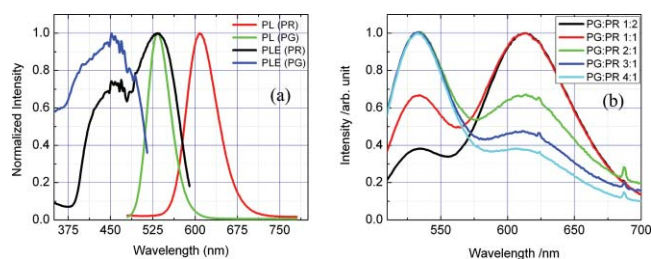


Fig. 5 (a) PL and PLE spectra from PG and PR phosphors and (b) PL spectra from mixtures of green and red phosphors (PG and PR). Legends show the weight ratio of green to red phosphors.

Table 1 Optical properties of phosphors.

Phosphor	QY (%)	Peak maximum (nm)	FWHM (nm)	CIE (λ_{Ex} :460 nm)
PG	77.9	535	~50	(0.280, 0.681)
PR	75.7	610	~65	(0.633, 0.366)

(R^2) of 0.99:

$$y = \frac{1.38}{x}. \quad (2)$$

The diminishing red intensities can be explained based on five concurrent effects: (i) for a change of weight ratio with a constant total weight of phosphor, intensity varies linearly with weight; (ii) difference in QYs of PG and PR (a linear dependence); (iii) absorption of green light by red phosphor (a nonlinear dependence); (iv) difference in particle size of red and green phosphor leads to different thickness and scattering effect (a nonlinear dependence); and (v) self-absorbed fraction of phosphor emissions (a linear dependence). If we ignore the fact that the combination of linear dependences could result in a nonlinear one and assume that scattering of incident light by the PG and PR is the same (refractive indices should be similar, because both the PG and PR phosphors are sulfo-selenide) and the thickness was constant for all samples, then absorption of green light by PR is the dominant nonlinear event responsible for the dependence shown in Eq. (2).

On the basis of this PL investigation on the effects of the weight ratios of the phosphors, the weight of the PG phosphor should be greater than or equal to the amount of PR in order to achieve high-quality white light. Lowering the amount of PG phosphor in the mixture compared to sample GR11 led not only to a shift of the CIE coordinates of downconverted light toward red but also reduced the overall efficiency. Therefore, GR11, GR 21, GR31, and GR41 samples were used for the downconversion of blue to white light.

5.3 Downconversion of Phosphor Mixture Using iLED

5.3.1 Luminescence spectra

Phosphor layers on the polished flat of encapsulated iLEDs were prepared using the procedure discussed in the sample-preparation section. Figure 6(a) shows the normalized downconversion luminescence spectra from samples prepared using the various mixtures of PG and PR phosphors in the PMMA-chlorobenzene solution. The luminescence spectra were acquired with the detector on the surface normal. The GR11 sample exhibited a red peak maximum that was 1.8 times higher than the green counterpart. Note that a mixture of PG and PR with a 1:1 weight ratio exhibited

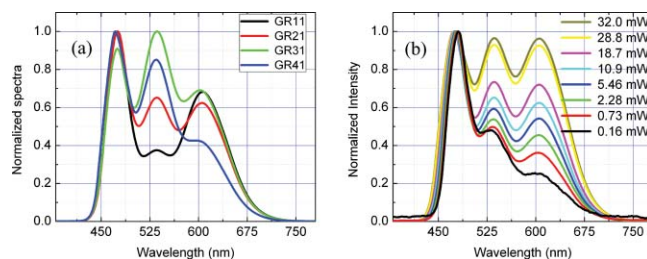


Fig. 6 (a) Normalized downconversion emission spectra of thin-film samples prepared using various weight ratios of PG to PR phosphors in a PMMA host at 4 mA. (b) Normalized downconverted white light from the sample PG21 versus power to the iLED.

Table 2 Ratio of PR to PG peak maxima for different samples excited with a monochromatized light (460 nm) versus iLED excitation.

Red to green peak maxima	Sample PG:PR 1:1	Sample PG:PR 2:1	Sample PG:PR 3:1	Sample PG:PR 4:1
PL	1.5	0.7	0.5	0.4
Downconversion	1.8	1.0	0.8	0.6

1.5 times enhancement under monochromatized excitation at 460 nm. Similarly, differences in intensity of red versus green peaks were found for all other samples, as tabulated in Table 2 (460-nm excitation).

Differences in the downconverted intensities for excitation by an iLED versus monochromatized light can be explained by differences in the excitation spectra of the two sources. In addition, there was variation of the emitted white light with iLED power, as shown in Fig. 6(b), which shows a nonlinear enhancement of red versus green peak maxima for sample GR21. Similar variations were also found for all the samples. Changes in the downconverted spectra were observed for yttrium–aluminum–garnet (YAG) phosphors using a blue iLED.¹⁷ Another investigation reported that the CCT changed with viewing angle for YAG downconverted white light.^{19,20} To further investigate, samples were prepared with only green (GR10) and red (GR01) phosphors in the PMMA host. Both samples exhibited spectral changes with diode power (not shown here). These nonlinear increases of peak maxima for red and green emissions were logarithmic with iLED power. Data from the normalized spectra with different power to iLED for each sample, and red and green phosphors showed different rates of enhancement with the iLED power. The spectral distribution stabilized at high power to the iLED, as shown in Fig. 6(b).

5.3.2 CIE color coordinates

The nonlinear changes of luminescence with power to the iLED caused shifts in the CIE coordinate and CRI values. The changes in CIE coordinates of white light produced from different phosphor layer compositions are shown in Fig. 7. Recall that changes in the CIE coordinates of pure blue light from the iLED with an increase in power so shown in Fig. 1(c). As discussed above, these changes were due to an increase of the FWHM and a shift of the peak position toward higher energies with increased iLED power. An ~ 2 nm change in wavelength has been reported for surface-mount InGaN devices.¹² A redshift of CIE coordinates was observed with increase in driving power to the iLEDs for phosphor samples GR11,

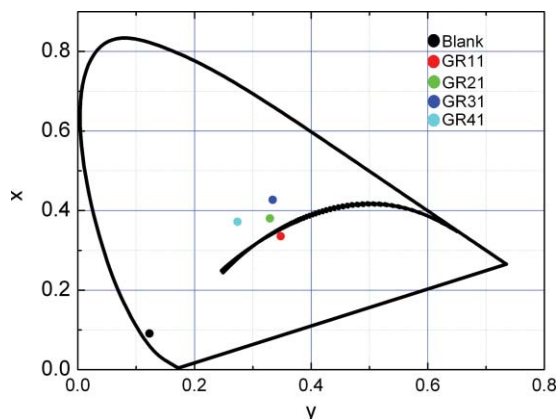
**Fig. 7** Color coordinates of downconverted white light from samples with different weight ratios of green to red phosphors.

Table 3 Ra, CIE coordinates and CCT values from different samples with different phosphor layer is at two different powers.

Sample	GR11		GR21		GR31		GR41	
Power (mW)	4.22	17.93	5.46	31.5	6.80	23.72	5.13	16.86
Ra	66	79	80	86	75	78	70	74
CIE	(0.370, 0.306)	(0.380, 0.301)	(0.347, 0.336)	(0.354, 0.327)	(0.331, 0.358)	(0.338, 0.353)	(0.263, 0.292)	(0.268, 0.290)
CCT			4856		5551	5285	11787	11305

GR21, GR31, and GR4, in agreement with changes in luminescence [an example is shown in Fig. 6(b)].

5.3.3 Color-rendering index of white light

The Ra value, which is an average CRI value from 15 standard colors, was calculated from the luminescent spectrum acquired along the surface normal for each device power. Table 3 shows the Ra values at two iLED currents for each sample, and the Ra increased with power for every sample. Figure 8 shows the CRI values for the 15 reference color standards²¹ (R1–R15) at different power from the four phosphor samples. For sample GR11, the CRI standard color values were between ~50 and 100, except for the R10 standard. Sample GR11 exhibited Ra values from 63 to 79 at low and high powers, respectively. The enhancement of Ra values with increased power is due to increased contribution at all standard colors, including the R10 value, as shown in Fig. 8(a). For sample GR21, the green component increased as compared to sample GR11. An Ra value of 86 was achieved power of 0.032 W to the iLED, although the CRI of the R9 standard was lower compared to the GR11 sample. The R9 CRI decreased as the green component increased for samples GR31 and GR41, as shown in Figs. 8(c) and 8(d), resulting in lower Ra values. The color temperature of the downconverted white light from sample GR21 was ~5000 K. As the concentration of green phosphor was increased, the color temperature increased to >11,000 K for sample GR41. The white light generated from YAG excited by a blue iLED exhibits low R9 CRI values.²² Kimura et al.¹² showed that the presence of a “valley”

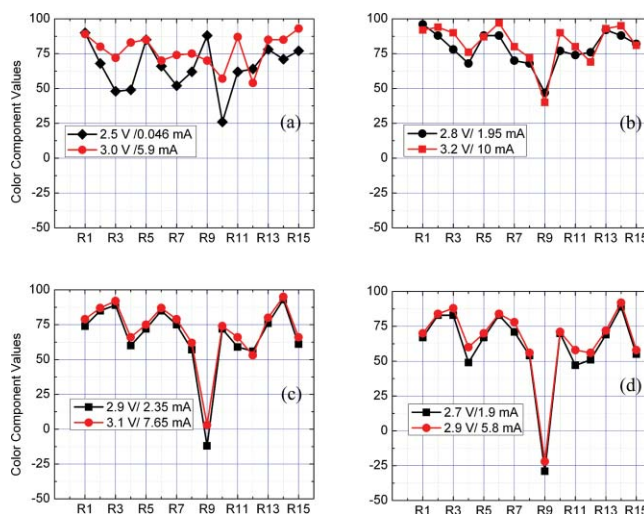


Fig. 8 Color-rendering index values of R1-R15 standard colors for sample (a) GR11, (b) GR21, (c) GR31, and (d) GR41. The maximum Ra value for GR11, GR21, GR31, and GR41 was 79, 86, 78, and 74, respectively.

between green and blue spectral regions significantly decreased the Ra value. It is expected that a larger intensity in the yellow region would increase the CRI values.

In order to test the effect of increased yellow intensity, downconversion phosphor layers were prepared using a red (peak maxima 641 nm and FWHM 55 nm) and a yellow (peak maxima 550 nm with FWHM 100 nm) emitting phosphors (Phosphor Technology, England) with similar photoluminescence quantum yields. The PL-PLE spectra showed (not shown here) that the PLE maximum of the red-emitting phosphor overlapped the PL emission peak from the yellow phosphor, indicating that emission from the yellow phosphor would be absorbed by the red phosphor. The (x,y) CIE color coordinates of the yellow and red phosphors were (0.46, 0.50) and (0.65, 0.30), respectively. The layers were prepared using different weight ratios of yellow to red phosphors in the PMMA host, and a weight ratio of 1:2 exhibited Ra values of 90 when the mixture was excited at monochromatized 460 nm, which is an acceptable value.¹⁹

5.4 Conversion Efficiency of Blue Light to White by Phosphor Mixtures

Luminance data (L) were collected from all samples using a PhotoResearch (PR650) camera. The luminance efficacy [φ , in lumens per watt] was calculated using Eq. (3) for phosphor-coated samples assuming Lambertian emission from the phosphor-film coated area ($A: 5 \times 10^{-5} \text{ m}^2$),

$$\varphi = \frac{L \times \pi \times A}{W}. \quad (3)$$

The sample GR00 produced highly directional blue light. Therefore, the efficiency was calculated without assuming Lambertian emission. The efficiencies (measured in lumens per watt) versus iLED power are plotted in Fig. 9. The data show that there is no improvement in the luminance efficacy for the blue iLED versus downconverted white light. The maximum luminance efficacy of white light was 10 lm/W for sample GR41, presumably due to both backscattering of blue and downconverted lights by the phosphor particles, low PL quantum yields of phosphors and quantum deficits between the blue excitation and the red and green emission. Previous research showed that the amount of reflected blue and downconverted light increased with an increased amount of phosphor in the downconversion layer.^{23,24} Kumura et al.¹² reported that combinations of blue iLED and bluish green, green, and red phosphors yielded low efficacy but high Ra values.

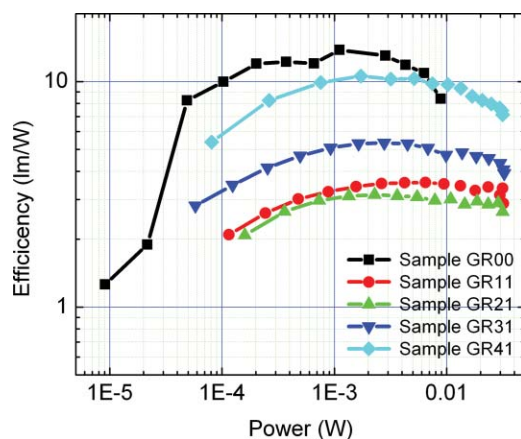


Fig. 9 Efficacy versus iLED power for different phosphor weight ratios.

6 Conclusions

Downconversion of blue light from an iLED to yield a high-quality white light was demonstrated using mixtures of red- and green-emitting phosphors in a PMMA host. A series of samples was prepared by varying the weight ratio of green to red phosphors. Good color temperatures (~ 5000 K) and average color-rendering indices (> 80) were achieved by optimizing the phosphor layer. However, the luminance efficacy was not improved by downconversion because of light scattering by the phosphor layer and Stoke's shift between the blue excitation and the red and green emissions.

Acknowledgments

This work was supported by the Department of Energy (DOE) Grant N. DE-FC26-06NT42855. We gratefully acknowledge supports in data collection and reduction by the staffs of the Major Analytical Instrumental Center, Materials Chemistry Characterization Laboratory, and Particle Engineering Research Center. We are also grateful for discussions with Dr. Franky So and Dr. Jaewon Lee. The authors are highly indebted to PhosphorTech, USA and Phosphor Technology, England for providing phosphor samples.

References

1. K. Bando, K. Sakano, Y. Noguchi, and Y. Shimizu, "Development of high-bright and pure-white LED lamps," *J. Light Visual Environ.* **22**, 2–5 (1998).
2. D. Bera, S. Maslov, L. Qian, and P. Holloway, "Synthesis of nanostructured Eu^{3+} -doped $\text{La}_2\text{O}_2\text{S}_2$ -based red-phosphor using combustion process," in *Proc. of IDRC 08*, pp. 221–223, SID, Orlando (2008).
3. A. A. Setlur, "Phosphor for LED-based solid-state lighting," *Interface* **18**, 32–36 (2009).
4. L. Chen, C.-C. Lin, C.-W. Yeh, and R.-S. Liu, "Light converting inorganic phosphors for white light-emitting diodes," *Materials* **3**, 2172–2195 (2010).
5. R. J. Xie and N. Hirosaki, "Silicon-based oxynitride and nitride phosphors for white LEDs—a review," *Sci. Technol. Adv. Mater.* **8**, 588–600 (2007).
6. W. Walter, "Optimum phosphor blends for fluorescent lamps," *Appl. Opt.* **10**, 1108–1113 (1971).
7. X. Guo, J. Graff, E. F. Schubert, and R. F. Schubert, "Photon recycling semiconductor light emitting diode," *Proc. SPIE* **3938**, 60–67 (2000).
8. W. J. Yang and T. M. Chen, " $\text{Ce}^{3+}/\text{Eu}^{2+}$ codoped Ba_2ZnS_3 : A blue radiation-converting phosphor for white light-emitting diodes," *Appl. Phys. Lett.* **90**, 171908 (2007).
9. R. J. Xie, N. Hirosaki, M. Mitomo, K. Takahashi, and K. Sakuma, "Highly efficient white-light-emitting diodes fabricated with short-wavelength yellow oxynitride phosphors," *Appl. Phys. Lett.* **88**, 101104 (2006).
10. F. Hide, P. Kozodoy, S. P. DenBaars, and A. J. Heeger, "White light from InGaN/conjugated polymer hybrid light-emitting diodes," *Appl. Phys. Lett.* **70**, 2664–2666 (1997).
11. A. R. Duggal, J. J. Shiang, C. M. Heller, and D. F. Foust, "Organic light-emitting devices for illumination quality white light," *Appl. Phys. Lett.* **80**, 3470–3472 (2002).
12. N. Kimura, K. Sakuma, S. Hirafune, K. Asano, N. Hirosaki, and R. J. Xie, "Extra high color rendering white light-emitting diode lamps using oxynitride and nitride phosphors excited by blue light-emitting diode," *Appl. Phys. Lett.* **90**, 051109 (2007).
13. Y. Gu and N. Narendran, "A non-contact method for determining junction temperature of phosphor-converted white LEDs," *Proc. SPIE* **5187**, 107–114 (2004).
14. S. Fujita and S. Tanabe, "Thermal Quenching of Ce^{3+} : $\text{Y}_3\text{Al}_5\text{O}_{12}$ Glass-Ceramic Phosphor," *Jpn. J. Appl. Phy.* **48**, 120210 (2009).
15. W. Chung, K. Park, H. J. Yu, J. Kim, B. H. Chun, and S. H. Kim, "White emission using mixtures of CdSe quantum dots and PMMA as a phosphor," *Opt. Mater.* **32**, 515–521 (2010).

16. H.-T. Li, C.-W. Hsu, and K.-C. Chen, "Enhancement of light efficiency of LED using a novel high refractive encapsulant," in *Proc. of Electronic Components and Technology Conference 2008*, Lake Buena Vista, FL, pp. 1926–1930 (2008).
17. R. Mueller-Mach, G. O. Mueller, M. R. Krames, and T. Trottier, "High-power phosphor-converted light-emitting diodes based on III-nitrides," *IEEE J. Sel. Top. Quantum Electron.* **8**, 339–345 (2002).
18. R. Kasuya, A. Kawano, and T. Isobe, "Characteristic optical properties of transparent color conversion film prepared from YAG:Ce³⁺ nanoparticles," *Appl. Phys. Lett.* **91**, 111916 (2007).
19. D. A. Steigerwald, J. C. Bhat, D. Collins, R. M. Fletcher, M. O. Holcomb, M. J. Ludowise, P. S. Martin, and S. L. Rudaz, "Illumination with solid state lighting technology," *IEEE J. Sel. Top. Quantum Electron.* **8**, 310–320 (2002).
20. M. R. Krames, J. B. D. Collins, N. F. Gardner, W. Gotz, C. H. Lowery, M. Ludowise, P. S. Martin, G. Mueller, R. Mueller-Mach, S. Rudaz, D. A. Steigerwald, S. A. Stockman, and J. J. Wierer, "High-power III-nitride emitters for solid-state lighting," *Phys. Status Solidi A* **192**, 237–245 (2002).
21. G. F. Ji and H. W. Shen, "Dynamic view selection for time-varying volumes," *IEEE Trans. Vis. Comput. Graphics* **12**, 1109–1116 (2006).
22. K. Sakuma, N. Hirotsuki, N. Kimura, M. Ohashi, R.-J. Xie, Y. Yamamoto, T. Suehiro, K. Asano, and D. Tanaka, "White light-emitting diode lamps using oxynitride and nitride phosphor materials," *IEICE Trans. Electron.* **E88-C**, 2057–2064 (2005).
23. N. Narendran, Y. Gu, J. P. Freyssonier-Nova, and Y. Zhu, "Extracting phosphor-scattered photons to improve white LED efficiency," *Phys. Status Solidi A* **202**, R60–R62 (2005).
24. K. Yamada, Y. Imai, and K. Ishi, "Optical simulation of light source devices composed of blue LEDs and YAG phosphor," *J. Light Visual Environ.* **27**, 70–74 (2003).

Debasis Bera was a postdoctoral associate in the Department of Materials Science and Engineering at the University of Florida. He is currently working at Philips Lumileds, San Jose, California. He received his BSc (Honors) in chemistry from Vidyasagar University, Midnapur, India, MSc in analytical chemistry from Jadavpur University, Kolkata, India, and MTech in materials science and engineering from Indian Institute of Technology Bombay, Mumbai, India. He received a PhD degree from the Department of Mechanical, Materials and Aerospace Engineering, University of Central Florida, Orlando, Florida. He has coauthored two book chapters, over 30 journal publication and one issued patent. He specializes on nanomaterials; optical materials; OLED, PLED, and LED downconversion; and white light.

Sergey Maslov received his BS in materials science and engineering from the University of Florida in 2005. His graduate work focused on a Department of Energy sponsored solid state lighting project in downconversion phosphors, and he was granted an MS in 2008. He is currently working for Intel in Arizona.

Lei Qian received the BS in physics from Zhengzhou University, MS from Henan University, and PhD from Beijing Jiaotong University, China. He is currently working as a postdoc in the Department of Materials Science and Engineering, University of Florida (UFL). Prior to joining UFL in 2006, he worked as research associate at AIST, Japan, on a mechanoluminescent sensor. He has coauthored two book chapters, over 40 journal publications, and two patents.

Paul H. Holloway is Distinguished Professor and the Ellis D. Verink, Jr. Professor of Materials Science and Engineering at the University of Florida, Gainesville. He is also the director of MICROFABRITECH, an interdisciplinary materials research program at the University of Florida. He received his PhD in 1972 from the Rensselaer Polytechnic Institute. He has also worked at General Electric and at Sandia National Laboratory. His areas of research include electrical contacts to semiconductors, optical emission from inorganic and organic thin films and powders, and synthesis and optical emission from nanophosphors.